Communication

Facile One-Step Synthesis of Highly Ordered Bimodal Mesoporous Phosphosilicate Monoliths

Liangming Xiong, Jianlin Shi, Lingxia Zhang, and Masayuki Nogami

J. Am. Chem. Soc., **2007**, 129 (39), 11878-11879• DOI: 10.1021/ja070466i • Publication Date (Web): 11 September 2007

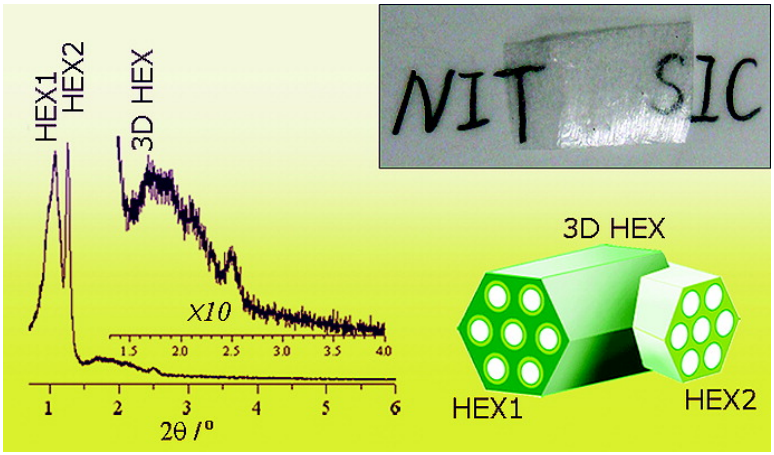

More About This Article

Additional resources and features associated with this article are available within the HTML version:

- Supporting Information
- Access to high resolution figures
- Links to articles and content related to this article
- Copyright permission to reproduce figures and/or text from this article

View the Full Text HTML

J|A|C|S
COMMUNICATIONS

Published on Web 09/11/2007

Facile One-Step Synthesis of Highly Ordered Bimodal Mesoporous Phosphosilicate Monoliths

Liangming Xiong,[†] Jianlin Shi,[‡] Lingxia Zhang,[‡] and Masayuki Nogami*,[†]

Department of Material Science and Engineering, Nagoya Institute of Technology, Nagoya, 466-8555, Japan, and Shanghai Institute of Ceramics, Chinese Academy of Sciences, Shanghai, 200050, China

Received January 27, 2007; E-mail: nogami@nitech.ac.jp

Ordered mesoporous materials (OMMs) are of particular interest in many fields because of their favorable structural properties,[1] and to meet some application requirements, their pore size must be controlled.[2] The mesopore sizes can be tuned by many methods,[2,3] but the methods could only enlarge the pore. Multiscale pores controlled independently with larger or smaller sizes and well-connected pores would be beneficial to some applications in, for example, catalysis.[4] Recently, bimodal mesoporous materials (BMMs) with pore connectivity received much attention,[4−6] because of their potentials in catalysis,[5a] separation,[4] and proton conduction.[5b,c]

Currently BMMs are mostly silica or carbon powders,[4,6] and their pores are well-connected, generally containing ordered mesopores connected by disordered pores at large mesoscales or microscales in the particle. Thus the BMM powders are very useful in heterogeneous catalysis[4] and absorption,[6] and the pore connectivity also makes them provide fast transfer pathways for guest molecules[4] and protons[5b] through the particle. The pathways may be further shortened and would work faster if they are bridged by regular mesopores. On the other hand, the development of BMMs into macrodimensions would give them particular potential in, for example, electrochemical[5c] and optical[7] devices. However, until now these kinds of bulk monolithic BMMs with well-connected regular pores have not been reported.

Herein, we present a facile method to synthesize ordered bimodal hexagonal mesoporous phosphosilicate monoliths (BHMPSMs). The monoliths were prepared in a sol−gel process, using pluronic P123 as a template and using tetraethoxysiliane (TEOS) and trimethoxyl phosphate (TMP) as additives. TMP was added 20 min later than TEOS to the solution of sample X-1. Sample X-1′ was prepared following the same process but using less TMP. The weight ratio of P/S of BHMPSMs is 0.101−0.188, determined by ICP−AES. For comparison, we prepared another phosphosilicate sample R1 by synchronously adding TEOS and TMP and a pure silica sample R2 without adding TMP. The experiment details are described in the Supporting Information (SI).

Figure 1a shows the small-angle X-ray diffraction (SAXRD) patterns of X-1, R1, and R2. It is easily seen that R1 and R2 have a similar diffraction characteristic: a 2D hexagonal structure with a space group *P6mm*, though the periodicity is not very high. The d_{100} spacing of R1 (∼7.48 nm) is larger than that of R2 (∼7.06 nm), implying that the simultaneously added TMP acted either as a dopant thickening the framework via hydrolysis and condensation or as a swelling agent enlarging the pores. However, X-1 has a different character, where at least 7 well-resolved peaks, p1−p7, can be observed with p2 being the strongest and sharpest. Their positions cannot fully match any unimodal mesostructure, but the reciprocal *d*-spacing values of p1, p4, and p5 follow the relationship $1:\sqrt{3}:2$ and those of p2, p6, and p7 also follow this relationship. This suggests that p1, p4, and p5 may be indexed as the (100), (110), and (200) reflections of a hexagonal system (labeled as HEX1), and p2, p6, and p7 can be indexed as the (100), (110), and (200) reflections of another hexagonal system (labeled as HEX2). It is clearly distinguished that HEX2 is more ordered and its unit cell is smaller ($d_{100} \approx 7.01$ nm) as compared with HEX1 ($d_{100} \approx 8.25$ nm), and both have a higher periodicity than R1 and R2. It should be noted that if both HEX1 and HEX2 were 2D hexagoanal, like R1 and R2, p3 would not match them still, suggesting that there would be a new phase whose resolution needs the more direct data. The other sample X-1′ exhibited similar inflections to that of X-1 (see SI), indicating this synthetic route is reproducible.

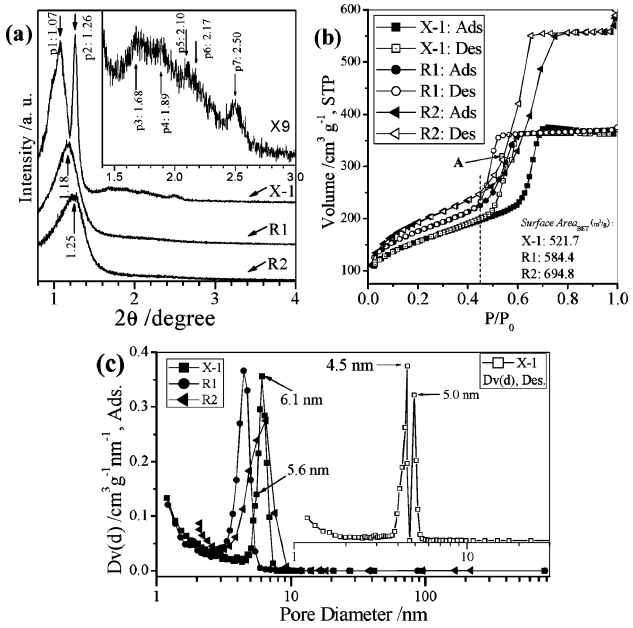

Figure 1. (a) SAXRD patterns, (b) N_2 sorption isotherms and BET surface areas of X-1, R1, and R2, and (c) their PSDs calculated from the adsorption branches. The inset shows the enlarged SAXRD pattern of X-1 in panel a and its PSD calculated from desorption branch in panel c.

All the N_2 sorption isotherms of X-1, R1, and R2 (Figure 1b) are of type IV character and show distinct capillary condensation and evaporation steps in the p/p_0 range 0.4−0.8. The pore volumes of X-1 and R1 are very close but evidently lower than that of R2. Despite that this is also true for the BET surface areas, there is still an evident difference between the surface areas of X-1 and R1, which is likely related to whether the samples were cracked or not (see SI). The desorption branch of X-1 presents a clear inflection at p/p_0 of 0.5−0.6 (point A), implying a possible dual porosity. Since all the hysteresis loops were closed at a p/p_0 of 0.41−0.48 along the desorption branch, a tensile strength effect (TSE) phenomenon might occur, resulting in a pore size distribution (PSD) peak at around 3.8 nm.[8] Thus PSD derived from the adsorption branch [denoted as PSD(Ads)], instead of that from the desorption branch [denoted as PSD(Des)], should be adopted to describe their

[†] Nagoya Institute of Technology.
[‡] Chinese Academy of Sciences.

10.1021/ja070466i CCC: $37.00

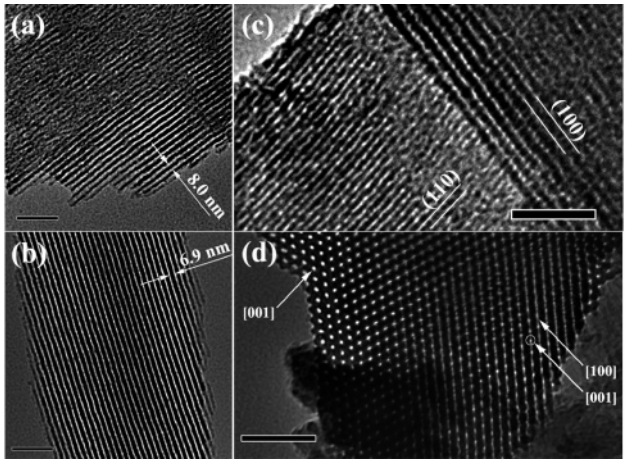

Figure 2. TEM images of X-1 having large (a) and small (b) spacing unit cells and pore-connected regions (c, d). All scale bars are 50 nm.

pore size, despite its lower resolution than that of the latter. Figure 1c gives their PSDs(Ads) with the Barrett−Joyner−Halender method and illustrates that both R1 and R2 have a unimodal PSD and the pore size of R1 (∼4.5 nm) is lower than that of R2 (∼ 6.5 nm). In combination with the XRD result, it can be concluded that the synchronously added TMP not only thickened the framework wall via hydrolysis and co-condensation but also shrank the pores, instead of acting as a swelling agent. For X-1, however, its PSD-(Ads) is very close to that of R2 but more narrow than the latter. Its PSD peak (∼6.1 nm) has a weak shoulder at around 5.6 nm. This can be confirmed by PSD(Des) (inset of Figure 1c), owing to its high resolution. The PSD(Des) curve presents 2 well-defined peaks, one at 4.5 nm and the other at 5.0 nm. The space between them is 0.5 nm, the same as that between the peak and its shoulder on the PSD(Ads) curve. No peak, derived from the TSE phenomenon,[8] occurs at around 3.8 nm. Thus, it is evident that X-1 is of bimodal mesostructures and its both PSDs are narrow but very close.

Transmission electron microscopy (TEM) observation can directly and effectively illustrate the bimodal structures of X-1. Figure 2a and b clearly give different single-crystal microdomains whose *d*-spacing are about 8.0 and 6.9 nm, respectively. That agrees well with the SAXRD result, where HEX1 is corresponding to the microdomain in Figure 2a and HEX2 is corresponding to that in Figure 2b. Moreover, the microdomain in Figure 2b is more periodic than that in Figure 2a, consistent with the XRD result. In addition, some pore networks were observed in Figure 2c and d. Figure 2c gives two sets of hexagonal channels intersecting in a [100] project, showing both (100) and (110) lattice fringes of a hexagonal phase. Figure 2d also gives two sets of hexagonal channels intersecting in a [001] project, showing both (001) and (100) pores. The concurrence of the pore networks in the [100] and [001] projects confirms the existence of 3D pore networks in X-1. Evidently, the 3D networks were formed in a mode like (HEX1 + HEX1) or (HEX2 + HEX2). Since that, it is also possible to form another 3D pore network in a mode like (HEX1 + HEX2) in X-1. Thus, p3 in the XRD pattern may be due to the (101) inflection of the latter 3D network. Besides these networks, some butt-jointing pores were observed (see SI).

On the basis of the above results, a formation mechanism of BHMPSM can be proposed, as shown in Scheme 1. Before the addition of TMP, mesostructured phases are formed following a hydrogen-bonding interaction mechanism, similar to that of SBA-15.[9] After the addition of TMP, a silicate rod assembly model may be available. The unassembled rods (I1) allow not only a further condensation of siliceous oligomers but also a co-condensation with

Scheme 1. The Proposed Formation Mechanism of BHMPSM

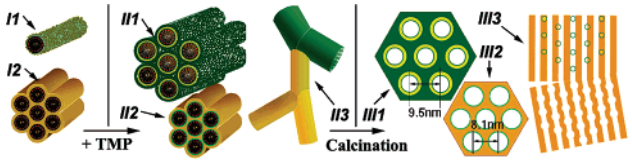

TMP and the diffusion of TMP and its hydrolysates into the siliceous network. Then the rods assemble and form HEX1 (II1, III1) with a large unit cell and thicker framework. For the well-assembled cells HEX2 (I2, II2, III2), TMP will not make them reassemble but can enter into the framework and entrance. The TMP there may not only keep well the ordering of the host structure[10] but also be hydrolyzed slowly and cross-condensed into the framework.[11] It is also possible for the neighboring cells, either HEX1 or HEX2, to be connected together by P−O−P or P−O−Si bonds formed in the co-condensation between the TMP's hydrolysates or between them and the siloxane matrix at the entrances, where the matrix is very active.[12] Thus, pore connectivity (II3, III3) may be formed at the ends of the cells. It may be also due to the pore connectivity that X-1 presents a glassy morphology containing fibrous patterns after calcination, different from that of R1. X-1 has a high proton conductivity (see SI), which, in a sense, implies its high pore connectivity.

In summary, we have proposed a simple method to prepare one glassy monolith with double highly ordered hexagonal mesotructures in a controllable manner. This monolith has dual narrow pore size distributions and pore connectivity and may find applications in absorption, separation, catalysis, and devices like fuel cells, sensors, and multiprocessors.

Acknowledgment. This work was supported by the COE Program in NITECH of Japan, NSFC (Grant No. 20633090), Shanghai Science Committee (Grant No. 0452nm056) of China, and *NGK* Spark Plug Co., Ltd.

Supporting Information Available: Experiment details, macromorphologies, XRD, TEM, EIS, and proton conductivity. This material is available free of charge via the Internet at http://pubs.acs.org.

References

(1) (a) Corma, A. *Chem. Rev.* **1997**, *97*, 2373. (b) Schüth, F.; Wingen, A.; Sauer, J. *Microporous Mesoporous Mater.* **2001**, *44*−*45*, 465. (c) Shi, J.-L.; Hua, Z.-L.; Zhang, L.-X. *J. Mater. Chem.* **2004**, *14*, 795.
(2) (a) Zhao, D.; Feng, J.; Huo, Q.; Melosh, N.; Fredrickson, G. H.; Chmelka, B. F.; Stucky, G. D. *Science* **1998**, *279*, 548. (b) Blin, J. L.; Su, B. L. *Langmuir* **2002**, *18*, 5303. (c) Sayari, A.; Hamoudi, S.; Yang, Y. *Chem. Mater.* **2005**, *17*, 212.
(3) (a) Khushalani, D.; Kuperman, A.; Ozin, G. A.; Tanaka, K.; Garces, J.; Olken, M. M.; Coombs, N. *Adv. Mater.* **1995**, *7*, 842. (b) Jansen, J. C.; Shan, Z.; Marchese, L.; Zhou, W.; von der Puil, N.; Maschmeyer, T. *Chem. Commun.* **2001**, 713.
(4) Sun, J.-H.; Shan, Z.; Maschmeyer, T.; Coppens, M.-O. *Langmuir* **2003**, *19*, 8395.
(5) (a) Yuan, Z.-Y.; Blin, J.-L.; Su, B.-L., *Chem. Commun.* **2002**, 504. (b) Mikhailenko, S.; Desplantier-Giscard, D.; Danumah, C.; Kaliaguine, S. *Microporous Mesoporous Mater.* **2002**, *52*, 29. (c) Yamada, M.; Li, D.; Honma, I.; Zhou, H. *J. Am. Chem. Soc.* **2005**, *127*, 13092.
(6) (a) Lu, A.-H.; Schmidt, W.; Spliethoff, B.; Schüth, F. *Adv. Mater.* **2003**, *15*, 1602. (b) Sun, J.; Shan, Z.; Maschmeyer, T.; Moulijn, J. A.; Coppens, M.-O. *Chem. Commun.* **2001**, 2670. (c) Lee, J.; Kim, J.; Hyeon, T. *Chem. Commun.* **2003**, 1138. (d) Huang, Y.; Cai, H.; Yu, T.; Zhang, F.; Zhang, F.; Meng, Y.; Gu, D.; Wan, Y.; Sun, X.; Tu, B.; Zhao, D. *Angew. Chem., Int. Ed.* **2007**, *46*, 1089.
(7) Gu, J.-L.; Shi, J.-L.; You, G.-J.; Xiong, L.-M.; Qian, S.-X.; Hua, Z.-L.; Chen, H.-R. *Adv. Mater.* **2005**, *17*, 557.
(8) Groen, J. C.; Louk. A. A. P.; Pérez-Ramírez, J. *Microporous Mesoporous Mater.* **2003**, *60*, 1.
(9) Wan, Y.; Shi, Y.; Zhao, D. *Chem. Commun.* **2007**, 897.
(10) Inagaki, S.; Guan, S.; Fukushima, Y.; Ohsuna, T.; Terasaki, O. *J. Am. Chem. Soc.* **1999**, *121*, 9611.
(11) Li, D.; Zhou, H.; Honma, I. *Nat. Mater.* **2004**, *3*, 65.
(12) Xiong, L.; Shi, J.; Gu, J.; Shen, W.; Dong, X.; Chen, H.; Zhang, L.; Gao, J.; Ruan, M. *Small* **2005**, *1*, 1044.

JA070466I